

Lifetime of the Be<sup>10</sup> 3.37-MeV Level. I. Experiment\*

E. K. WARBURTON, D. E. ALBURGER, AND D. H. WILKINSON†

*Brookhaven National Laboratory, Upton, New York*

(Received 2 October 1962)

Collective effects in  $E2$  transitions are found even in light nuclei. We have sought to extend the knowledge of this phenomenon by measuring the lifetime of the  $2^+$  first excited state of Be<sup>10</sup> at 3.37 MeV. To do this we have used two new variants of the Doppler-shift attenuation method. The Be<sup>10</sup> was produced by the Be<sup>9</sup>( $d,p$ )Be<sup>10</sup> reaction and the recoiling Be<sup>10</sup> was slowed down in beryllium or in beryllium-copper. We find a mean lifetime of  $(1.4 \pm 0.3) \times 10^{-13}$  sec. The analysis of Doppler-shift measurements of the type used here is given at length.

## I. INTRODUCTION

ELECTRIC quadrupole transitions in light nuclei form an interesting study. Although the independent-particle model in intermediate coupling gives an acceptable account of the level schemes and dipole transitions of the light nuclei, it has long been recognized that it fails rather badly and systematically for the  $E2$  transitions in that these are usually several times faster than the theory predicts. It is important to pursue this phenomenon, very well known in heavier nuclei, to as light nuclei as possible and to study transitions between states for which the independent-particle model gives an otherwise-satisfactory account. It is also obviously important that the transition studied should be one for which the model does not predict a speed that varies rapidly with the parameters of the model. The transition from the first excited state of Be<sup>10</sup> fulfills all these conditions admirably as is shown in the following paper.<sup>1</sup>

The  $J^\pi = 2^+$  first excited state of Be<sup>10</sup> at 3.37 MeV is known<sup>2</sup> to decay by  $\gamma$  emission to the  $J^\pi = 0^+$  Be<sup>10</sup> ground state. Using a nuclear radius constant of 1.2 F, the Weisskopf estimate<sup>3</sup> for the mean lifetime of this  $E2$  transition is  $\tau = 1.4 \times 10^{-12}$  sec. Experimentally, it is found that in the light nuclei the most likely  $E2$  speed is about 5 times the Weisskopf estimate with an uncertainty of roughly a factor of five either way.<sup>3</sup> Without recourse to a theoretical calculation the best estimate is that the Be<sup>10</sup> 3.37-MeV level has a mean lifetime within a factor of 5 of  $3 \times 10^{-13}$  sec. Since this is just the interval expected for the slowing down time of light nuclei in solids, experimental methods which depend on the ratio of this time to the mean lifetime of Be<sup>10</sup> should be applicable to a measurement of the latter.

There have been two previous attempts to measure the lifetime of the Be<sup>10</sup> first excited state, both of which

utilized methods of this sort. The first,<sup>4</sup> which used the Doppler-shift attenuation method,<sup>5-7</sup> resulted in a 50% confidence limit,  $\tau < 3 \times 10^{-13}$  sec. The second attempt<sup>8</sup> was an investigation of the spread in angle of the recoiling Be<sup>10</sup> nuclei counted in coincidence with protons emitted at a fixed angle to the beam following the Be<sup>9</sup>( $d,p$ )Be<sup>10\*</sup> reaction, the spread in angle being partially due to the emission of  $\gamma$  radiation by the recoiling nuclei and consequently dependent on the ratio of the lifetime to the slowing down time of the recoiling nuclei. This attempt yielded  $\tau < 8 \times 10^{-14}$  sec where the limit corresponds to one standard deviation from the measured effect.

We have used two new variations of the Doppler-shift attenuation method in a successful attempt to measure the lifetime of the Be<sup>10</sup> first excited state. The next section contains a review of the essentials of the Doppler-shift method and a discussion of the two variants used in this experiment.

Historically, the largest part of the uncertainty in the measurements of nuclear lifetimes by the Doppler-shift method has been due to inexact knowledge of the range-velocity relationship. Recent measurements have extended the knowledge and accuracy of this relationship considerably and it is expected that further range-velocity data will be forthcoming. These data are accurate enough at the present time to justify a more elaborate analysis of Doppler-shift measurements than was called for in the past. An analysis of the present Doppler-shift measurements which makes full use of the available range-velocity data is described in Sec. III.

## II. DOPPLER-SHIFT ATTENUATION

The energy  $E$  of the  $\gamma$  radiation emitted from nuclei formed at time  $t=0$  and moving thereafter with velocity  $v(t)$ , or  $c\beta(t)$ , is given by

$$E = E_0[1 + \beta(t) \cos\theta] \quad (1)$$

<sup>4</sup> D. Kohler, California Institute of Technology thesis, unpublished (1959).

<sup>5</sup> S. Devons, G. Manning, and D. St. P. Bunbury, Proc. Phys. Soc. (London) **A68**, 18 (1955).

<sup>6</sup> D. St. P. Bunbury, S. Devons, G. Manning, and J. H. Towle, Proc. Phys. Soc. (London) **A69**, 165 (1956); S. Devons, G. Manning, and J. H. Towle, *ibid.*, **A69**, 173 (1956).

<sup>7</sup> E. Bashandy, Nucl. Instr. and Methods **12**, 227 (1961).

<sup>8</sup> A. H. Boyarkina and A. F. Tulinov, Soviet Phys.—JETP **9**, 244 (1959).

\* Work performed under the auspices of the U. S. Atomic Energy Commission.

† Permanent address: Nuclear Physics Laboratory, Oxford, England.

<sup>1</sup> E. K. Warburton, D. E. Alburger, D. H. Wilkinson, and J. M. Soper, following paper, Phys. Rev. **129**, 2191 (1963).

<sup>2</sup> F. Ajzenberg-Selove and T. Lauritsen, Nucl. Phys. **11**, 1 (1959).

<sup>3</sup> D. H. Wilkinson, in *Nuclear Spectroscopy*, edited by F. Ajzenberg-Selove (Academic Press Inc., New York, 1960), Part B, pp. 852-889.

for  $\beta(t) \ll 1$ . In Eq. (1)  $E_0$  is the  $\gamma$ -radiation energy for nuclei at rest and  $\theta$  is the angle of emission of the  $\gamma$  rays relative to  $\beta(t)$ . If recoiling nuclei are slowed down and stopped in a material, then the average energy of the  $\gamma$  radiation will be

$$E = E_0[1 + \beta(0)F' \cos\theta], \quad (2)$$

where

$$F' = \frac{\lambda}{\beta(0)} \int_0^\infty \beta(t) e^{-\lambda t} dt, \quad \lambda = \tau^{-1}, \quad (3)$$

if scattering of the recoiling nuclei is negligible as is usually the case. Essentially, the Doppler-shift attenuation method is to measure  $F'$  for a single stopping material, or a relationship between  $F'$  values for several different stopping materials. Since  $F'$  depends on the ratio of the nuclear lifetime to the slowing down time of the nuclei in the material, a knowledge of the latter allows  $\tau$  to be determined from a measurement of  $F'$ . For instance, in many cases the range of the recoiling nuclei in a given material can be represented by  $R = \alpha c\beta(t)$ . In this case,  $\alpha$  is the slowing down time, i.e., the time for the velocity to decrease to  $e^{-1}$  of its initial value, and

$$F'[\text{for } R = \alpha c\beta(t)] \equiv F = \frac{\lambda\alpha}{1 + \lambda\alpha}, \quad \text{or} \quad \lambda\alpha = \frac{F}{1 - F}. \quad (4)$$

Usually the difference in  $\gamma$ -ray energy is measured for two values of  $F'$  (i.e., two stopping materials) or for two values of  $\theta$ . Then, if  $\Delta E$  is the shift in  $\gamma$ -ray energy,

$$F_1' - F_2' = \frac{\Delta E}{E_0\beta(0) \cos\theta} \quad (5)$$

where  $\sigma(\theta_{c.m.})$  is the differential cross section for emission of  $m_3$  per unit solid angle at  $\theta_{c.m.}$ . In this case the average energy of the  $\gamma$  radiation will still be given by Eq. (2) but with  $\beta(0)$  replaced by its average value  $\beta_i(E)$ , with  $\theta$  now representing the angle of the  $\gamma$  radiation to the beam and with the assumption that  $F'$  is independent of  $\beta(0)$  as in Eq. (4). One or another of the many possible variations<sup>5</sup> of these two methods of defining the average velocity of the recoiling nuclei have been used in previous Doppler-shift measurements.

The particle-gamma coincidence method was used in the previous attempt<sup>4</sup> to measure the Be<sup>10</sup> 3.37-MeV level lifetime by the Doppler-shift attenuation method. The Be<sup>9</sup>( $d,p$ )Be<sup>10</sup> reaction with 3-MeV deuterons and a thin (10  $\mu\text{g}/\text{cm}^2$ ) Be<sup>9</sup> target was used. This method was limited by two factors: (1) the low particle-gamma coincidence yield, and (2) the large background of C<sup>13</sup> 3.09-MeV  $\gamma$  rays from C<sup>13</sup> contamination of the target.

In order to circumvent these problems we devised two variants of the Doppler-shift method which can be

performed using thick targets (for which the C<sup>12</sup> contamination is not a problem) and either singles spectra (first method) or gamma-gamma coincidence spectra (second method). For observation of the  $\gamma$  radiation alone using a target thick enough to stop the beam the  $\beta(0)$  of Eq. (2) is replaced by

$$F' = \frac{\Delta E}{E_0\beta(0)(\cos\theta_1 - \cos\theta_2)} \quad (6)$$

in the first case, and

in the second case. Generally, the excited nuclei  $M_4^*$  are formed in a reaction of the type  $M_2(m_1, m_3)M_4^*$ , and for a given incident energy of the particles  $m_1$  there is a continuum of  $\beta(0)$  given by

$$\beta(0) = \beta_{c.m.}[1 - \gamma^{-1} \cos\theta_{c.m.}], \quad (7)$$

where  $c\beta_{c.m.}$  is the speed of the center-of-mass in the laboratory system,  $\gamma$  is the ratio of the speed of the center-of-mass in the laboratory system to the speed of the recoiling nuclei in the center-of-mass system, and  $\theta_{c.m.}$  is the angle to the beam of the particles  $m_3$  in the center-of-mass system (i.e.,  $180^\circ - \theta_{c.m.}$  is the angle of the recoiling nuclei to the beam in the center-of-mass system).

One of the practical problems which must be overcome in the conventional use of the Doppler-shift method is to define the value of  $\beta(0)$ , or an average value of  $\beta(0)$ , to use in conjunction with Eqs. (2) and (3) in a determination of  $F'$ . One of the usual ways is to observe the  $\gamma$  radiation in coincidence with the particles  $m_3$ , the latter being detected at a definite angle to the beam. In this way  $\beta(0)$  is determined uniquely by the kinematics of the reaction.

Alternately, if the angular distribution of the particles  $m_3$  is known and the angular correlation between the  $\gamma$  radiation and  $M_4$  can be neglected, then the average value of  $\beta(0)$  which we designate by  $\beta_i(E)$  is given by

$$\beta_i(E) = \beta_{c.m.} \frac{\int_{-1}^{+1} [1 - \gamma^{-1} \cos\theta_{c.m.}] \sigma(\theta_{c.m.}) d(\cos\theta_{c.m.})}{\int_{-1}^{+1} \sigma(\theta_{c.m.}) d(\cos\theta_{c.m.})}, \quad (8)$$

performed using thick targets (for which the C<sup>12</sup> contamination is not a problem) and either singles spectra (first method) or gamma-gamma coincidence spectra (second method). For observation of the  $\gamma$  radiation alone using a target thick enough to stop the beam the  $\beta(0)$  of Eq. (2) is replaced by

$$\langle \beta_i \rangle = \int_0^{E_{m_1}} \sigma(E) \left( \frac{dE}{dx} \right)^{-1} \beta_i(E) dE / \int_0^{E_{m_1}} \sigma(E) \left( \frac{dE}{dx} \right)^{-1} dE, \quad (9)$$

where  $E_{m_1}$  is the bombarding energy,  $\sigma(E)$  is the total cross section for formation of  $M_4^*$  at a bombarding energy  $E$ ,  $dE/dx$  is the stopping power of the target for the bombarding particle, and  $\beta_i(E)$  is given by Eq. (8). In Eq. (9) the angular correlation between the  $\gamma$  radiation and the recoiling nuclei is assumed to be negligible.

In general, the angular distribution data needed to evaluate  $\langle\beta_i\rangle$  accurately from Eqs. (8) and (9) are not available. Also the correction of Eq. (9) for the angular correlation of the  $\gamma$  rays with  $M_4$  would sometimes be quite difficult to assess. Thus, it is desirable to find means of measuring  $F'$ , or a relation between  $F'$  values, that are as independent of  $\langle\beta_i\rangle$  as possible (first method) or alternatively a method of defining  $\langle\beta_i\rangle$  more directly (second method).

In the first method the energy difference  $\Delta E$  of the  $\gamma$  radiation measured at two angles,  $\theta_1$  and  $\theta_2$ , to the beam is measured for two thick targets having different slowing down times for the recoiling nuclei but both containing some fraction of the target nuclei homogeneously incorporated. Then the ratio of the  $F'$  values for these two targets will be given by

$$R_{F'} = F'_1/F'_2 = \frac{\langle\beta_i\rangle_2 (\Delta E)_1}{\langle\beta_i\rangle_1 (\Delta E)_2}. \quad (10)$$

The average speed of the recoiling nuclei will not necessarily be the same in the two materials (i.e.,  $\langle\beta_i\rangle_1 \neq \langle\beta_i\rangle_2$ ) since the stopping power  $dE/dx$  of the two targets for the bombarding particles,  $m_1$ , will not necessarily be proportional to each other [see Eq. (9)]. However, it turns out in practice that  $\langle\beta_i\rangle_1 \cong \langle\beta_i\rangle_2$  to a very good approximation and the difference can be corrected for by using Eq. (9) with a quite rough knowledge of  $\sigma(E)$  and  $\beta_i(E)$ .

For  $R = \alpha c \beta(t)$ ,  $F'$  is independent of the speed of the recoiling nuclei [see Eq. (4)]. We shall see that the range-velocity relationship is not linear but close enough so that an iterative correction can be made for the deviation, which introduces a dependence of  $F'$  on  $\beta(0)$ . Then the measurement of  $(\Delta E)_1$  and  $(\Delta E)_2$  can be made to yield a value for the ratio  $R_F$  given by

$$R_F = \frac{\lambda\alpha_1}{1 + \lambda\alpha_1} \frac{1 + \lambda\alpha_2}{\lambda\alpha_2}. \quad (11)$$

If we now define  $f$  as  $\alpha_2/\alpha_1$ , we have

$$\lambda\alpha_1 = \frac{fR_F - 1}{f(1 - R_F)}. \quad (12)$$

The second method can be used when the nuclear state for which a lifetime measurement is desired is fed by a  $\gamma$ -ray cascade from a higher state and it is known that the lifetime of the higher state is very much shorter than the slowing-down time, i.e.,  $F' = 1$  for this state. We designate these successive  $\gamma$  rays by  $\gamma_1$  and  $\gamma_2$ . If the Doppler shift of  $\gamma_1$  is measured between two angles to the beam and the shift of  $\gamma_2$ , detected in coincidence with  $\gamma_1$ , is measured for the same two angles, then from Eq. (6)

$$F' = (E_1/E_2)(\Delta E_2/\Delta E_1). \quad (13)$$

In this method  $\langle\beta_i\rangle$  has been determined by measuring  $\Delta E_1$ . This method strictly depends on the isotropy of the  $m_3 - \gamma_1$  angular correlation.

In actual practice  $F'$  is measured from the difference in Doppler shifts of  $\gamma_1$  and  $\gamma_2$ . For instance,  $\Delta E_1$  is measured and in an independent measurement the gain is adjusted between observations at the two angles so that the apparent shift  $\Delta E_2$  is zero. Under these conditions the relationship between  $F'$  and the apparent shift of  $\gamma_1$ , designated by  $\Delta E_1'$ , is

$$F' = 1 - \Delta E_1'/\Delta E_1 \quad (14)$$

since, in general,  $\Delta E_1' = \Delta E_1 - (E_1/E_2)\Delta E_2$ .

### III. DOPPLER-SHIFT MEASUREMENTS

The  $\text{Be}^9(d,p)\text{Be}^{10}$  reaction, which has a  $Q$  value of 4.590 MeV, was used in the two Doppler-shift methods of measuring the lifetime of the  $\text{Be}^{10}$  3.37-MeV level. For the first method the thick targets consisted of beryllium metal and of a copper-beryllium alloy (hereinafter designated as Cu-Be) containing 15 at. % of Be. The Cu-Be target was used for the gamma-gamma coincidence method.

In the more commonly used Doppler-shift technique, a single target is bombarded and the gamma-ray energy is measured at various angles with respect to the beam by moving the detector. An essential feature of our first experiment, as shown in Fig. 1, is that the detector remains in a fixed position and two target positions are provided in order that gamma rays may be measured at forward or at backward angles.<sup>9</sup> This scheme avoids the type of gain changes often encountered in moving NaI detectors. The design of the target holders is such that in position 1 either the Be or Cu-Be target may be bombarded or alternatively the beam may be allowed to pass on to target position 2. For detection of the gamma rays a 5 in.  $\times$  5 in. NaI crystal was used together with a CBS 7817 photomultiplier tube. Since the 7817 tube has a small rate-dependent gain and since the radiations from the targets are not isotropic the requirement of high gain stability was met by the following procedures. Paraffin was placed on both sides of the counter so as to reduce the background due to neutrons

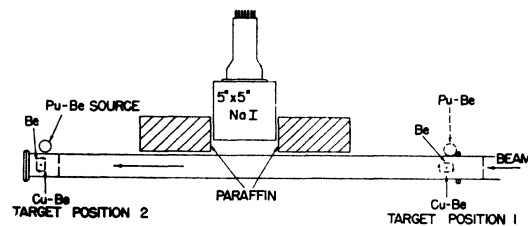


FIG. 1. Experimental arrangement for measuring Doppler shifts of gamma rays from  $\text{Be}^9 + d$  reactions. The NaI(Tl) crystal has an average angle of  $17^\circ$  to the beam for target position 1 and  $163^\circ$  for target position 2.

<sup>9</sup> This method was suggested by Rubby Sherr.

(which is more severe when observing in the forward direction). The NaI detector was placed slightly closer to target position 2 such that the total counting rate of the crystal was the same when using either target position. Finally, a radioactive Pu-Be source, which emits gamma rays of 4.43 MeV, was used not only for establishing a reference line in the pulse-height spectrum but for stabilizing the photomultiplier gain by means of a circuit due to de Waard.<sup>10</sup> Assuming that the Pu-Be source were to be kept in a fixed position with respect to the detector a possible source of error in our technique would be that the efficiency of the NaI crystal might depend on the direction of the incident gamma rays. To check this effect for the conditions of the experiment the Pu-Be source was placed near target position 1 and a thorium source (2.62-MeV gamma ray) was placed alternately near target position 2 and beside the Pu-Be source. Within the accuracy of the measurement ( $\pm 0.1\%$ ) no dependence of the gain on the position of the thorium source was discernible. Nevertheless, the Pu-Be source was always placed near the target being bombarded in the positions indicated in Fig. 1.

The average angles of the  $\gamma$ -ray detector to the beam were  $17^\circ$  (target position 1) and  $163^\circ$  (target position 2). These angles were found by averaging  $\cos\theta$  over the detector area by numerical integration. For the arrangement of Fig. 1, then,  $\cos\theta_1 - \cos\theta_2 = 1.91 \pm 0.01$ . The uncertainty in this value includes an estimate of the possible effect of a nonisotropic distribution of the  $\gamma$  transitions of interest relative to the deuteron beam.

The Doppler shifts of the  $\text{Be}^{10}$  5.96  $\rightarrow$  0 and 3.37  $\rightarrow$  0 transitions were investigated with the arrangement of Fig. 1. The 5.96-MeV  $\gamma$  ray was measured by using two 4-mg/cm<sup>2</sup> Be targets and a deuteron energy of 3.1 MeV. The deuteron energy loss in a 4-mg/cm<sup>2</sup> Be target is 0.73 MeV at this energy. This measurement was made for three reasons: (1) A knowledge of the Doppler shift of this  $\gamma$  ray for the target thickness and deuteron energy used was desirable for an interpretation of measurements<sup>11</sup> made on the  $\gamma$  rays from  $\text{Be}^9 + d$  using an intermediate-image magnetic-lens pair spectrometer. (2) The  $\text{Be}^{10}$  5.96-MeV level has  $J^\pi = 1^-$  and can, therefore, decay by  $E1$  emission to the  $\text{Be}^{10}$  0<sup>+</sup> ground state and 2<sup>+</sup> 3.37-MeV level.<sup>2</sup> Thus, it is expected that  $\tau \ll 10^{-13}$  sec for this level and this is assumed. In this case, and under the conditions of the present bombardment,  $F' = 1$  for this level and the Doppler shift measurement amounted to a measurement of  $\langle\beta_i\rangle$  for the  $\text{Be}^9(d,p)\text{Be}^{10}$  (5.96-MeV level) reaction. Enough information on the angular distribution and the yield versus deuteron energy of the  $\text{Be}^9(d,p)\text{Be}^{10}$  (5.96-MeV level) reaction is available so that  $\langle\beta_i\rangle$  can be calculated fairly accurately from the kinematics of the reaction. Thus, this measurement serves as a check on our ex-

perimental method. (3) The  $\text{Be}^{10}$  5.96  $\rightarrow$  3.37  $\rightarrow$  0 cascade was used to obtain the 3.37-MeV lifetime by the gamma-gamma coincidence method. Thus,  $\Delta E_1$  of Eq. (14) can be obtained from a Doppler shift measurement of the  $\text{Be}^{10}$  5.96-MeV  $\gamma$ -ray.

Spectra showing the full-energy-loss peak of the  $\text{Be}^{10}$  5.96-MeV  $\gamma$  ray and the  $\text{C}^{14}$  4.43-MeV  $\gamma$  ray were taken alternately with the two target positions. Six spectra were taken for each target. A typical set is shown in Fig. 2. The background has been partially removed from the spectra of Fig. 2 by subtracting 1600 counts/channel from the  $17^\circ$  spectrum and 1000 counts/channel from the  $163^\circ$  spectrum. This background is mainly due to neutrons from the  $\text{Be}^9(d,n)\text{B}^{10}$  reaction. The two 4.43-MeV full-energy-loss peaks shown in Fig. 2 have been normalized by a slight adjustment of the intensity of the  $163^\circ$  spectrum. The 12 spectra were recorded with a bias of 4.0 MeV (320 channels).

From a comparison of the two spectra shown in Fig. 2 the Doppler shift of the 5.96-MeV  $\gamma$  ray is seen to be about 8 channels. To evaluate the Doppler shift from the 12 spectra, each spectrum was plotted logarithmically on large-scale semitransparent graph paper and for each set the shift of the 4.43-MeV peaks were determined by laying one plot on top of the other and adjusting the graph paper until the peaks coincided as well as could be determined by eye. Then the difference in channel numbers of the two spectra was read off the graphs. The procedure was then repeated for the 5.96-MeV peaks. It is felt that the shift could be determined with an uncertainty of about 0.3 channel by this procedure. The small gain changes observed between runs were compensated for by multiplying the shift of the 4.43-MeV peak by 5.96/4.43 and subtracting the result from the shift of the 5.96-MeV peak. The six values of

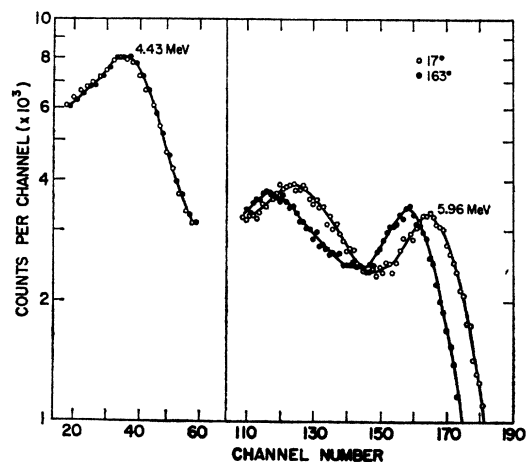


Fig. 2. The full-energy and "one-escape" peaks of the  $\text{Be}^{10}$  5.96-MeV gamma ray and the full-energy peak of the  $\text{C}^{14}$  4.43-MeV gamma ray, obtained with the arrangement of Fig. 1 using two 4-mg/cm<sup>2</sup>  $\text{Be}^9$  targets and  $E_d = 3.1$  MeV. The two spectra were recorded with a pulse-height analyzer bias of 320 channels (4.0 MeV).

<sup>10</sup> H. de Waard, *Nucleonics* **13**, 36 (1955).

<sup>11</sup> E. K. Warburton, D. E. Alburger, and D. H. Wilkinson (to be published).

the shift determined in this manner were consistent with each other and yielded an average of  $7.78 \pm 0.35$  channels, where the internal error is given. The gain control effected by the stabilizer circuit was such that the largest shift of the 4.43-MeV peak between the  $17^\circ$  and  $163^\circ$  spectra was  $+0.6$  channel and the average shift was  $+0.06$  channel so that the measured Doppler shift of the 5.96-MeV line is essentially the same as it would have been if the 4.43-MeV peak had been used only for stabilization and not as an energy reference line.

The shift of the 5.96-MeV line in keV corresponding to  $7.78 \pm 0.35$  channels is  $95.6 \pm 4.3$  keV, the uncertainty is increased somewhat to take account of possible systematic errors, and using  $\cos\theta_1 - \cos\theta_2 = 1.91$ , a shift of  $50 \pm 3.5$  keV between  $0^\circ$  and  $90^\circ$  is obtained. Thus, for this experiment,  $\langle\beta_i\rangle = (0.84 \pm 0.06) \times 10^{-2}$ .

The threshold for the  $\text{Be}^9(d,p)\text{Be}^{10}$  (5.96-MeV level) reaction is 1.67 MeV. Excitation functions have been obtained for the yield of the 5.96- and 3.37-MeV  $\gamma$  rays from  $\text{Be}^9+d$  from  $E_d = 1.0$  to 5.5 MeV.<sup>12</sup> Angular distributions for the  $\text{Be}^9(d,p)\text{Be}^{10}$  (5.96-MeV level) reaction have been measured<sup>13</sup> at  $E_d = 2.5$  and 2.9 MeV and an excitation curve for the protons from this reaction emitted at a laboratory angle of  $20^\circ$  from  $E_d = 2.0$  to 3.05 MeV has also been determined.<sup>13</sup> The angular distributions have the form expected for an  $l_n = 0$  stripping pattern as is the case for this level at higher deuteron energies.<sup>2</sup> Thus, stripping is the predominant reaction mechanism and because of the zero-orbital angular momentum of the captured neutron in the stripping process there will be no correlation between the  $\text{Be}^{10}$  recoils and the emitted  $\gamma$  radiation insofar as the reaction proceeds by stripping. Thus,  $\beta_i(E)$  can be calculated from the angular distribution of the outgoing protons. From the angular distributions,  $\beta_i(E)$  is determined to be  $0.795 \times 10^{-2}$  and  $0.790 \times 10^{-2}$ , respectively, at  $E_d = 2.9$  and 2.5 MeV. From the excitation curves a fairly good extrapolation of  $\beta_i(E)$  can be made from the apparent threshold ( $E_d \approx 1.9$  MeV) to  $E_d = 3.1$  MeV. Between 2.1 and 3.1 MeV it appears that  $\beta_i(E) = (0.79 \pm 0.05) \times 10^{-2}$ , so that  $\langle\beta_i\rangle = (0.79 \pm 0.05) \times 10^{-2}$  for a target of any thickness and for incident deuteron energies in the range  $2.4 < E_d < 3.1$  MeV since the yield for  $E_d < 2.1$  is practically negligible. Thus, our measured value for  $\langle\beta_i\rangle$  agrees with that expected from the kinematics of the reaction.

The Doppler shift of the  $\text{Be}^{10}$  3.37-MeV level was next investigated using the experimental arrangement of Fig. 1. A 2.8-MeV deuteron beam bombarded targets of Be and Cu-Be which were infinitely thick for 2.8-MeV deuterons. Since the ratio of the shifts in Be and Cu-Be was desired, a full set of spectra consisted of spectra for both targets at each angle, four spectra in all. The measurements consisted of three sequences of 8, 4, and 14 sets, respectively. The three sequences were

<sup>12</sup> J. H. McCrary, T. W. Bonner, and A. H. Ranken, Phys. Rev. **108**, 392 (1957).

<sup>13</sup> L. F. Chase, Jr. (to be published).

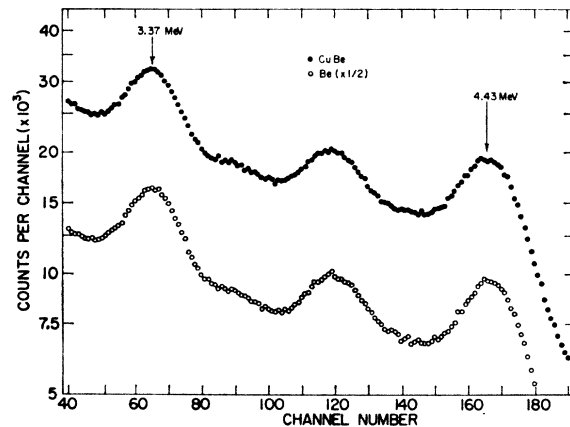


Fig. 3. The full-energy and "one-escape" peaks of the  $\text{C}^{12}$  4.43-MeV gamma ray and the "full-energy" peak of the  $\text{Be}^{10}$  3.37-MeV gamma ray obtained with the arrangement of Fig. 1 with the target at position 1 and a deuteron beam of 2.8 MeV incident on thick targets of Be (open circles) and Cu-Be (closed circles). The spectra were recorded with a pulse-height analyzer bias of 260 channels (2.7 MeV).

taken under slightly different conditions and the last was a good deal more accurate than the first two because of the experience gained in these preliminary runs.

Figure 3 shows two typical spectra from the last sequence of sets. These spectra were obtained at  $17^\circ$  to the beam. The 4.43-MeV reference peak, its "one-escape" peak, and the 3.37-MeV full-energy-loss peak can be seen. In the last sequence the spectra were recorded with a bias of 260 channels or 2.7 MeV. The deuteron beam intensity was adjusted when the targets were changed so that the counting rate stayed constant. The beam intensity was  $\sim 0.04 \mu\text{A}$  for the Be target and  $\sim 0.1 \mu\text{A}$  for the Cu-Be target, where the ratio of beam currents reflects the relative yields from the two targets and is consistent with their known compositions. The background from the Cu-Be target was slightly higher than for the pure Be target; however, there was no noticeable structure in this background above a  $\gamma$ -ray energy of 1 MeV.

The spectra were analyzed to obtain  $(\Delta E)_{\text{Cu}}$  and  $(\Delta E)_{\text{Be}}$  in the same way as the  $\text{Be}^{10}$  5.96-MeV  $\gamma$ -ray data were analyzed. For the last sequence it was felt that the shift of either the 4.43- or 3.37-MeV peak could be read from the graph paper with an accuracy of 0.1–0.2 channels.

The values of  $(\Delta E)_{\text{Cu}}/(\Delta E)_{\text{Be}}$  obtained from the three sequences were  $0.84 \pm 0.09$ ,  $0.76 \pm 0.12$ , and  $0.81 \pm 0.028$  where the uncertainty is the internal error. A value of  $0.81 \pm 0.028$  is adopted. The average values of  $(\Delta E)_{\text{Cu}}$  and  $(\Delta E)_{\text{Be}}$  were  $26.9 \pm 0.8$  and  $33.3 \pm 0.6$  keV, respectively. From the latter two values we get

$$F_{\text{Cu}} \langle\beta_i\rangle_{\text{Cu}} = (0.417 \pm 0.013) \times 10^{-2}$$

and

$$F_{\text{Be}} \langle\beta_i\rangle_{\text{Be}} = (0.518 \pm 0.01) \times 10^{-2}.$$

We now estimate  $\langle\beta_i\rangle_{\text{Cu}}/\langle\beta_i\rangle_{\text{Be}}$  in order to obtain  $R_F'$  ( $=F_{\text{Cu}}'/F_{\text{Be}}'$ ) from  $(\Delta E)_{\text{Cu}}/(\Delta E)_{\text{Be}}$  as defined in Eq. (10). The data which are available for an estimate of  $\langle\beta_i\rangle$  are the 3.37-MeV  $\gamma$ -ray yield curve of McCrary *et al.*,<sup>12</sup> complete proton angular distributions at seven deuteron energies between 0.3 and 0.9 MeV,<sup>14</sup> proton angular distributions for the forward hemisphere at  $E_d = 3.5, 3.0$  and 2.5 MeV,<sup>15</sup> relative proton cross sections at  $150^\circ$  and  $160^\circ$  for  $E_d = 3.0$  MeV,<sup>4</sup> and gamma-proton angular correlations at  $E_d = 3.5, 3.0$  and 2.5 MeV.<sup>15</sup> The value of  $\langle\beta_i\rangle$  obtained for the  $\text{Be}^{10}$  5.96-MeV level, the  $\text{Be}^{10}$  5.96-MeV  $\gamma$ -ray yield curve,<sup>12</sup> and the branching ratio of the  $\text{Be}^{10}$  5.96-MeV level,<sup>2,11</sup> are also necessary since a considerable fraction of the 3.37-MeV  $\gamma$ -ray yield is due to the decay of the 5.96-MeV level. Also there are accurate  $dE/dx$  data<sup>16</sup> for protons in Be and Cu. From these data  $\langle\beta_i\rangle$  can be estimated accurately enough for present purposes by estimating  $\beta_i(E)$  and integrating Eq. (9) numerically. The result is  $\langle\beta_i\rangle_{\text{Cu}}/\langle\beta_i\rangle_{\text{Be}} = 0.993 \pm 0.002$  so that  $R_F' = 0.816 \pm 0.028$ . The correction is practically negligible. From this analysis we also obtain  $\langle\beta_i\rangle = (0.67 \pm 0.1) \times 10^{-2}$  for both targets. These data will be analyzed to obtain a lifetime estimate in the next section.

The arrangement of Fig. 4 was set up for use with the gamma-gamma coincidence variation of the Doppler-shift method which we note to be applicable because of the lack of correlations due to the  $l=0$  stripping mechanism. The desire for as high a gamma-gamma coincidence rate as possible motivated the change to a single target position, and thus a movable  $\gamma$ -ray detector, and also the use of poor target-crystal geometry. Spectra were taken with the movable crystal in the two positions shown. As before, the angle of the detector to the deuteron beam was determined by averaging  $\cos\theta$  over the detector area. The result was  $\theta_1 = 15^\circ$ , and  $\theta_2 = 143^\circ$ , with  $\cos\theta_1 - \cos\theta_2 = 1.78 \pm 0.01$ . The deuteron beam energy was 2.75 MeV. The Cu-Be was infinitely thick for this deuteron energy.

A singles spectrum is shown in the lower curve (open circles) of Fig. 5. Similar spectra were observed in the fixed 5-in.  $\times$  5-in. crystal shown in Fig. 4, and a coincidence gate was set on the output from this crystal as shown in Fig. 5. This gate included most of the "one-escape" peak of the 3.37-MeV  $\gamma$  ray as well as part of the "two-escape" peak and Compton distribution from the  $\gamma$  ray. It also included the full-energy-loss peak of the 2.59-MeV  $\gamma$  ray from the  $\text{Be}^{10}$  5.96  $\rightarrow$  3.37 transition. A spectrum observed in coincidence with this gate in the movable crystal, which was at  $143^\circ$  to the beam in this case, is shown in the upper curve (closed circles) of Fig. 5. The enhancement of the 2.59- and 3.37-MeV full-energy-loss peaks is apparent. The gate was chosen so that the areas under these two peaks would be

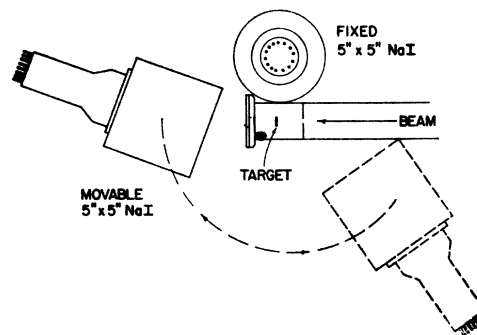


FIG. 4. Experimental arrangement for measuring Doppler shifts by the gamma-gamma coincidence method. The movable NaI crystal has average angles to the beam of  $15^\circ$  and  $143^\circ$  for the two positions shown.

approximately equal. The coincidence spectrum of Fig. 5 has an approximately 20% contribution from random coincidences. The Doppler-shift measurement consisted of recording two such spectra, one with the movable crystal at  $15^\circ$  to the beam and one with it at  $143^\circ$ . For these spectra and gain stabilizer received its feedback signal from the  $\text{Be}^{10}$  3.37-MeV full-energy-loss peak. Eight measurements of the relative Doppler shift of the  $\text{Be}^{10}$  2.59- and 3.37-MeV  $\gamma$  rays were obtained in three sequences using this technique. The spectra were taken with an analyzer bias of about 255 channels (2.1 MeV), the bias varied slightly from set to set.

The relative shift of the two peaks was determined graphically in the same manner as in the measurements described previously. With the gain of the two spectra (i.e.,  $\theta = 15^\circ$  and  $143^\circ$ ) normalized so that the 3.37-MeV peak shift was zero, the shift of the 2.59-MeV peak was about 1.5 channels. The average of the eight measurements gave a value for the shift of the 2.59-MeV line (with the 3.37-MeV line held constant) of  $\Delta E_1' = 11.9 \pm 1.6$  keV [see Eq. (14)]. In obtaining this result a correction was applied to the measurement for the contribution of randoms to the spectrum. The relative contribution of random coincidences could be estimated from the spectral shape since the  $\text{B}^{10}$  2.86-MeV  $\gamma$  ray from  $\text{B}^{10}$  3.58  $\rightarrow$  0.72 (see Fig. 5) was not in coincidence with the coincidence gate which was set on the fixed crystal spectra. The correction was obtained from the relation  $\Delta E_1' = \Delta E_1 - (E_1/E_2)\Delta E_2$  [see discussion of Eq. (14)] using the value of  $37.8 \pm 0.8$  keV adopted for  $\Delta E_1$  (see below), and the value of  $\Delta E_2$  obtained for 3.37-MeV  $\gamma$  rays in Cu-Be from the first method with a correction applied for the different geometries of Figs. 1 and 4. From these data we get  $18.6 \pm 1.0$  keV for the apparent shift of the 2.59-MeV peak with the 3.37-MeV peak (random contribution) held constant. The correction amounted to an average of about 1 keV due to an average 15% random contribution of the 3.37-MeV  $\gamma$  ray.

Because of the much poorer statistics necessitated by the low coincidence counting rate, the shift could not

<sup>14</sup> I. Resnick and S. S. Hanna, *Phys. Rev.* **82**, 463 (1951).

<sup>15</sup> S. A. Cox and R. M. Williamson, *Phys. Rev.* **105**, 1799 (1957).

<sup>16</sup> W. Whaling, in *Handbuch der Physik*, edited by S. Flügge (Springer-Verlag, Berlin, 1957), Vol. 34, p. 193.

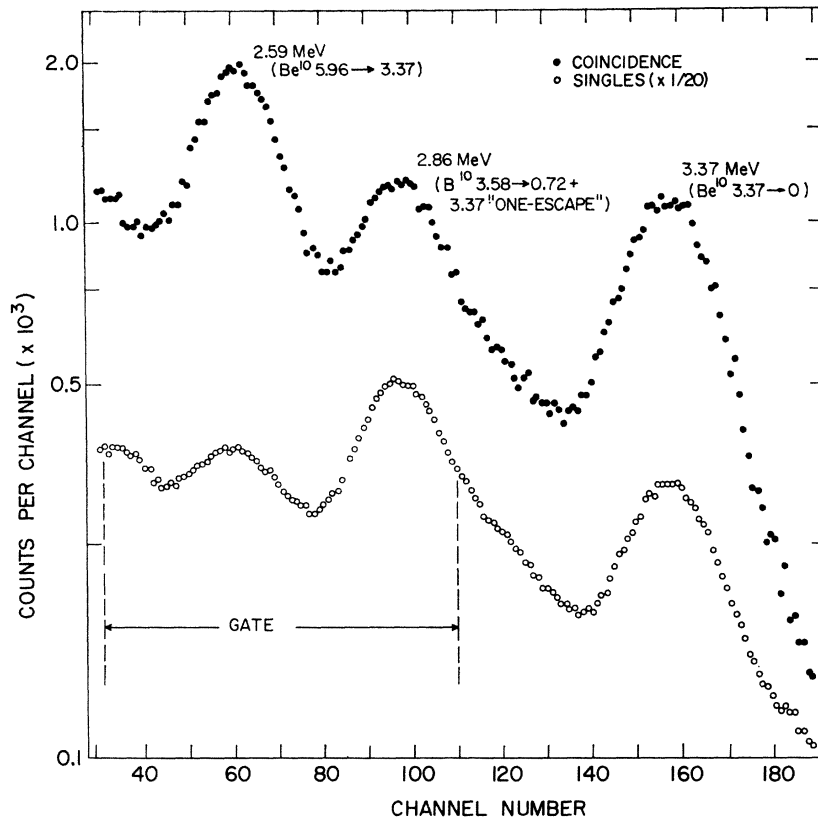


FIG. 5. Spectra obtained using the arrangement of Fig. 4, with a 2.75-MeV deuteron beam incident on a thick Cu-Be target and the movable NaI crystal at  $143^\circ$  to the beam. The open circles shown are singles spectrum from the movable crystal while the closed circles shown are a coincidence spectrum with the movable crystal gated by the fixed crystal. The spectra were taken with an analyzer bias of 255 channels (2.1 MeV).

be obtained as accurately by graphical analysis as was the case for the single spectra of the first method. In that case it was felt that the accuracy of the graphical analysis was as good as a numerical method such as determining centroid shifts or a curve-fitting program. For the coincidence spectra, however, it was felt that numerical analysis would be inherently more accurate and so the shifts were determined by subtracting background from the Gaussian (assumed) peaks and finding the centroid of the remainder. This method had the advantage that it yielded an estimate of the external error. The average shift ( $\Delta E_1'$ ) of the 2.59-MeV peak determined in this manner was  $10.8 \pm 0.9$  keV, where the correction for randoms has been applied. The internal error is given, the external error was estimated to be  $\pm 0.8$  keV. Averaging this result with the result obtained by graphical analysis gives  $\Delta E_1' = 11.2 \pm 0.9$  keV.

We now need the Doppler shift of the 2.59-MeV  $\gamma$  ray for the same target-crystal arrangement in order to obtain  $F_{Cu}'$  from our measurement of  $\Delta E_1'$ . This could be obtained from our previous measurement of the  $Be^{10}$  5.95-MeV  $\gamma$ -ray Doppler shift since the fractional shifts of the 5.96- and 2.59-MeV  $\gamma$  rays must be the same in the absence of proton-gamma angular correlations which we expect to be the case on account of the  $l=0$  stripping mechanism. However, as a check, the Doppler shift of the 5.96-MeV  $\gamma$  ray was measured again using the

arrangement of Fig. 4 and with a deuteron energy of 2.75 MeV bombarding a Be target. Three spectra were taken alternately at each angle with the 4.43-MeV line of Pu-Be as a reference peak. The result was  $91 \pm 6$  keV corresponding to  $51 \pm 4$  keV for the shift between  $0^\circ$  and  $90^\circ$ . This checks with the measurement of 3.1 MeV from which  $50 \pm 3.5$  keV was obtained using the arrangement of Fig. 1. Averaging these two values with the shift of  $47 \pm 2$  keV obtained from consideration of the proton angular distributions gives  $49 \pm 2$  keV from which we obtain  $\Delta E = (1.78 \pm 0.01)(2.59/5.96)(49 \pm 2) = 37.8 \pm 0.8$  keV as the shift of the  $Be^{10}$  2.59-MeV  $\gamma$  ray for the same conditions under which  $\Delta E_1' = 11.2 \pm 0.9$  keV was obtained. Then, from Eq. (14), we have

$$F_{Cu}' = 1 - (11.2 \pm 0.9)/(37.8 \pm 0.8) = 0.694 \pm 0.024.$$

This result will be analyzed in the next section together with the result obtained by the first method to obtain two independent estimates of the lifetime of the  $Be^{10}$  3.37-MeV level.

#### IV. RANGE-VELOCITY RELATIONSHIPS AND THE ANALYSIS OF THE DOPPLER-SHIFT MEASUREMENTS

The first task to be considered in this section is that of obtaining as accurately as possible, the range-velocity relationships for  $Be^{10}$  nuclei in Cu and in Be. Once these data are available, the results of the last

section can be analyzed to obtain the Be<sup>10</sup> 3.37-MeV level transition probability ( $\lambda$ ) or mean lifetime ( $\tau$ ).

The available range-velocity data which we shall use are contained in the compilation of Whaling,<sup>16</sup> the  $dE/dx$  data of Porat and Ramavataram,<sup>17-19</sup> and the range-energy data of Powers and Whaling.<sup>20</sup>

There are no experimental data for the range or stopping power of Be ions in Cu and Be and so we must interpolate from the data available for the ranges and stopping power of other ions on various stopping materials. Following Porat and Ramavataram<sup>17-19</sup> we use Bohr's orbital velocity  $\beta_0$  ( $=1/137$ ) as a convenient velocity unit in the following discussion. For the present experiments the largest possible value of  $\beta(t)$  is  $2.5\beta_0$  in the first method and  $2.0\beta_0$  in the second method; thus we are interested in range-velocity relationships for  $\beta(t) < 2.5\beta_0$ . In Fig. 6 are shown the stopping power versus velocity data of Porat and Ramavataram<sup>17-19</sup> for various ions in nickel. Note that  $v/v_0 \equiv \beta/\beta_0$ . These authors also obtain similar data for He<sup>4</sup>, C<sup>12</sup>, O<sup>16</sup>, and Ne<sup>20</sup> incident on C, Al, Ag, and Au with  $v/v_0 \gtrsim 1$ . These data indicate that for  $1.0 < v/v_0 < 2.0$ ,  $dE/dx$  is proportional to  $v/v_0$  to a very good approximation.

In the velocity range we are considering, the stopping power  $dE/dx$  is made up of an electronic contribution  $(dE/dx)_e$  and a nuclear contribution  $(dE/dx)_n$ . Powers and Whaling<sup>20</sup> quote the following theoretical estimates for  $(dE/dx)_e$  and  $(dE/dx)_n$ :

$$-(dE/dx)_e = \frac{8\pi N Z_1^{7/6} Z_0 \hbar^3 v}{m_0 e^2 (Z_1^{2/3} + Z_0^{2/3})^{3/2}}, \quad (15a)$$

$$-(dE/dx)_n = \frac{4\pi N Z_1^2 Z_0^2 e^4}{M_0 v^2} \ln \frac{a M_0 M_1 v^2}{(M_0 + M_1) Z_0 Z_1 e^2}. \quad (15b)$$

Equation (15a) is due to Lindhard and Scharff,<sup>21</sup> while Eq. (15b) is due to Bohr.<sup>22</sup> In Eq. (15),  $N$  is in atoms/cm<sup>3</sup>,  $Z_1$  and  $M_1$  refer to the moving ion,  $Z_0$  and  $M_0$  to the stopping material, and  $m_0$  and  $e$  to the electron. The screening parameter  $a$  is given by

$$a = 0.885 (\hbar^2 / m_0 e^2) (Z_0^{2/3} + Z_1^{2/3})^{-1/2}.$$

For the ions and stopping material we are considering,  $(dE/dx)_n < 0.1(dE/dx)_e$  for  $v/v_0 > 1$ ; thus Eq. (15) predicts  $(dE/dx) \cong K v/v_0$  for  $1 < v/v_0 < 2$  as is observed by Porat and Ramavataram<sup>17-19</sup> (Fig. 6).

Powers and Whaling found that  $dE/dx$  evaluated from Eq. (15) agreed with experiment within the experimental uncertainty of  $\pm 10\%$  for their data for Ne

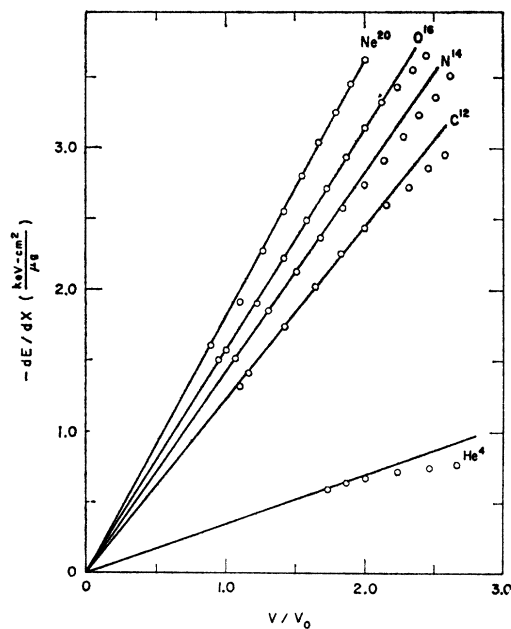


FIG. 6. Energy loss vs velocity (in units of  $c/137$ ) for He<sup>4</sup>, C<sup>12</sup>, N<sup>14</sup>, O<sup>16</sup>, and Ne<sup>20</sup> ions in Be metal. The data are those of Porat and Ramavataram (references 17, 18 and 19).

ions in Be in the velocity interval  $0.44 < v/v_0 < 1$  and gave values 10–15% higher than their data for N ions in Be in the velocity interval they investigated,  $0.5 < v/v_0 < 1.23$ . Thus, Eq. (15) seems to be a quite good representation of  $(dE/dx)$  for  $0.5 < v/v_0 < 2$  and we feel we can use it with confidence to interpolate available data to obtain information on the stopping of Be<sup>10</sup> ions in Cu and Be.

As a first step we find the proportionality constant  $K$  for Be ions in Ni by interpolating the data of Fig. 6. Note that Eq. (15a) is independent of the mass  $M_1$  of the moving ion. The information used in the interpolation is shown in Fig. 7. The experimental points are obtained from the slopes of the straight lines shown in Fig. 6, and have an uncertainty of less than 5%.<sup>17-19</sup> The additional point at  $Z=1$  is estimated from data given by Whaling.<sup>16</sup> The lowest (dashed) curve in Fig. 7 is a plot of Eq. (15a), which can be put in the form  $(dE/dx)_e = K_e v/v_0$  with

$$K_e = 11.60 \left( \frac{Z_0}{A} \right) \frac{Z_1^{7/6}}{(Z_0^{2/3} + Z_1^{2/3})^{3/2}} \frac{\text{keV-cm}^2}{\mu\text{g}}, \quad (16)$$

where  $A$  is the atomic weight of the stopping material.

The middle curve of Fig. 7 is a plot of Eq. (15), i.e.,  $(dE/dx)_e + (dE/dx)_n$ , and the upper (solid) curve is Eq. (15) normalized to the experimental points for  $Z=6-10$ . From Fig. 7 we obtain a value for  $K$  of  $0.78 \pm 0.04$  keV-cm<sup>2</sup>/μg for Be ions in Ni. Equation (16) can be used to convert this value into one for Be ions in Cu with small additional error since the relevant

<sup>17</sup> D. I. Porat and K. Ramavataram, Proc. Roy. Soc. (London) **A252**, 394 (1959).

<sup>18</sup> D. I. Porat and K. Ramavataram, Proc. Phys. Soc. (London) **77**, 97 (1961).

<sup>19</sup> D. I. Porat and K. Ramavataram, Proc. Phys. Soc. (London) **78**, 1135 (1961).

<sup>20</sup> D. Powers and W. Whaling, Phys. Rev. **126**, 61 (1962).

<sup>21</sup> J. Lindhard and M. Scharff, Phys. Rev. **124**, 128 (1961).

<sup>22</sup> N. Bohr, Kgl. Danske Videnskab. Selskab, Mat.-Fys. Medd. **18**, No. 8 (1948).



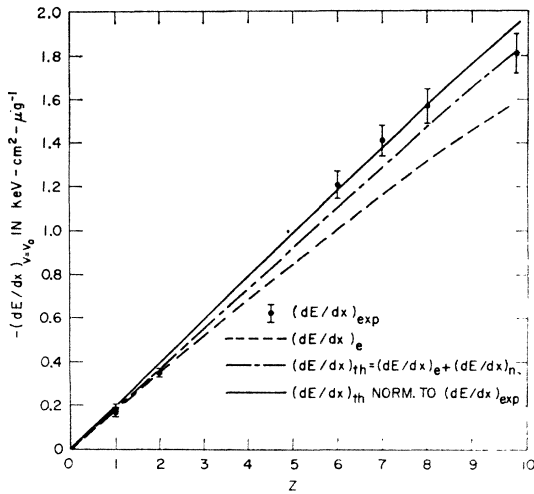


FIG. 7. The energy loss of ions in nickel for an ion velocity  $v=v_0$ . The experimental points are from data of Porat and Ramavaram (references 17, 18 and 19) except for that at  $Z=1$  which is from data given in reference 16. The theoretical curves are explained in the text.

properties of Ni and Cu are quite similar. The result is  $K(\text{Be}^{10} \text{ in Cu}) = (0.75 \pm 0.04) \text{ keV-cm}^2/\mu\text{g}$ .

If the experimental data for  $dE/dx$  are represented by  $dE/dx = Kv/v_0$  for  $1 < v/v_0 < 2$ , then the range for the same velocity interval must be given by

$$R(\mu\text{g}/\text{cm}^2) = (M_1 v_0^2 / K)(v/v_0 - v_n/v_0). \quad (17)$$

Equation (17) follows from the relation

$$R = R(E_1) + \int_{E_1}^E \frac{dE}{dE/dx} = R(v_1) + \int_{v_1}^v \frac{M_1 v dv}{dE/dx}. \quad (18)$$

The data of Powers and Whaling for the ranges of N and Ne ions in Be and C and of N ions in Al have the form of Eq. (17) for  $v/v_0 > 0.6$ , and for stopping in C and Al the ranges are in good agreement with those extracted from the  $dE/dx$  data of Porat and Ramavaram. This is illustrated in Fig. 8 which shows the range data of Powers and Whaling for N ions in Al and Be. The straight line fitted to the Al data has a slope  $M_1 v_0^2 / K$  with  $K$  obtained from the  $dE/dx$  data.<sup>19</sup> This fit illustrates that the range and stopping power data are in agreement.

The straight line fitted to the data for N in Be shown in Fig. 8 was used to extract a value of  $M_1 v_0^2 / K$  and thus  $K$ . In a similar manner a value of  $K$  was obtained for Ne in Be. These data were used to interpolate in  $Z$  to obtain a value of  $K$  for  $\text{Be}^{10}$  ions in Be. The information used in the interpolation is shown in Fig. 9. The experimental points for protons and alphas in Be were estimated from data given in the compilation of Whaling.<sup>16</sup> The curves have the same meaning as those in Fig. 7. From Fig. 9 we obtain a value of  $K$  for  $\text{Be}^{10}$  on Be of  $(2.3 \pm 0.15) \text{ keV-cm}^2/\mu\text{g}$ .

A value of  $K$  for the Cu-Be target can now be obtained by converting the  $K$  values to stopping power per atom and combining the values for Cu and Be according to the ratio of atomic percent (i.e., 85% Cu, 15% Be). The result is  $K(\text{Be}^{10} \text{ on Cu-Be}) = (0.79 \pm 0.04) \text{ keV-cm}^2/\mu\text{g}$ .

Two different forms were used for the range vs velocity relationship. These were

$$R = \alpha(v - v_n), \quad v > v_n \\ = 0, \quad v \leq v_n \quad (19)$$

and

$$R = \alpha[v - (2/\pi)v_n \tan^{-1}(\pi/2 v/v_n)]. \quad (20)$$

The first of these implies that  $-dE/dx$  is infinite for  $v < v_n$  and proportional to  $v$  for  $v > v_n$ . The second implies that

$$-(dE/dx) = \frac{K_n}{(v/v_0)} + K_e(v/v_0), \quad (21)$$

and is an attempt to reproduce the theoretical form of  $dE/dx$  [Eq. (15)]. The two expressions for  $R$  are shown fitted to the data for N in Be in Fig. 8. The straight line is Eq. (19) while the dashed curve is Eq. (20). It is seen that the latter fits the data quite well. Equations (19) and (20) both give values for the Doppler-shift attenuation factor of the form,

$$F' = [\lambda\alpha / (1 + \lambda\alpha)][1 - \delta(v_i/v_n)], \quad (22)$$

where  $v_i$  is the initial velocity of the moving ion. For

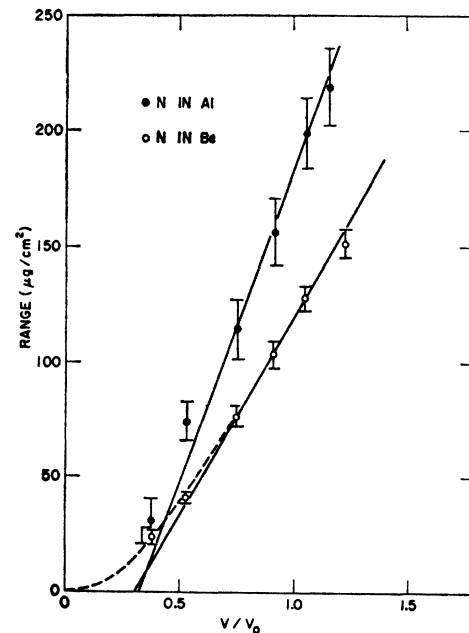


FIG. 8. Range-velocity relationships for N ions in Al and Be. The data are those of Powers and Whaling (reference 20). The fits to the data are explained in the text.

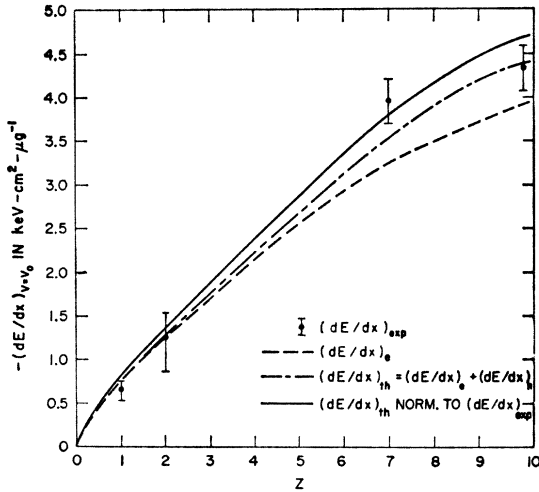


FIG. 9. The energy loss in Be for an ion velocity  $v=v_0$ . The experimental points for  $Z=7$  (N ions) and  $Z=10$  (Ne ions) are from data of Powers and Whaling (reference 20). The experimental points for  $Z=1$  (protons) and  $Z=4$  (He ions) are from data given in reference 16. The theoretical curves are explained in the text.

Eq. (19)  $\delta$  is given by

$$\delta(v_i/v_n) = (v_n/v_i)^{\lambda\alpha+1}, \quad (23)$$

while for Eq. (20), with  $\gamma_i = (\pi/2)v_i/v_n$ , we have

$$\delta(\gamma_i) = \frac{1}{\gamma_i(1+\gamma_i^2)^{\lambda\alpha/2}} \int_0^{\tan^{-1}\gamma_i} \frac{d\theta}{(\cos\theta)^{\lambda\alpha}}. \quad (24)$$

The integral can be evaluated for integral values of  $\lambda\alpha$  and  $\delta(\gamma_i)$  can then be plotted against  $\lambda\alpha$  for various values of  $\gamma_i$ . In Fig. 10  $\delta(\gamma_i)$  is shown for 4 values of  $\gamma_i$ .

As can be seen from Fig. 6, the proportionality between  $dE/dx$  and  $v/v_0$  begins to break down for  $v/v_0 > 2.0$ . This does not influence the second method for which  $\beta \leq 2.0\beta_0$ , but for the first method we have  $\beta \leq 2.5\beta_0$  so that use of Eq. (19) or (20) will introduce some error into the analysis of the first method. However, in the first method only a small percentage of the Be<sup>10</sup> recoil have  $\beta > 2.0$  and mainly for this reason the error resulting from use of Eq. (19) or (20) can be neglected compared to other uncertainties.

For  $\lambda\alpha \gg 1$  or  $v_i/v_n \gg 1$  the two forms of the range vs velocity relationship lead to approximately equal and small values of  $\delta$ ; however, for either  $\lambda\alpha \lesssim 1$  or  $v_i/v_n \lesssim 2$  the correction factor  $\delta$  is quite large (see Fig. 10) and that due to Eq. (19) is considerably larger than that for Eq. (20). In the present experiment  $v_i/v_0$  varies from 0.25 to 2.5 while  $v_n/v_0$  is about 0.3 thus it is rather important to obtain  $\delta$  as accurately as possible. For this reason Eq. (20) was used even though the analysis is simpler using Eq. (19). Also, Eq. (20) appears to give a good representation of the range-velocity data and the theoretical expression for  $dE/dx$  can be used as a guide

in obtaining the constant  $v_n$ —which is presumed to be dependent on the ratio of  $(dE/dx)_n$  to  $(dE/dx)_e$ .

The following procedure was used to obtain the constants  $\alpha$  and  $v_n$  in Eq. (20). The constant  $K_n$  was determined by fitting  $K_n/(v/v_0)$  from Eq. (21) to the theoretical expression for  $(dE/dx)_n$ . Then  $v_n/v_0$  was determined from the relation between Eqs. (20) and (21):

$$v_n/v_0 = (\pi/2)(K_n/K_e)^{1/2}. \quad (25)$$

This gave  $v_n/v_0 = 0.3$  for Be in Be and 0.4 for Be in Cu. Next the slope  $dR/dv$  of Eq. (20) was set equal to  $M_{1v_0}/K$  at  $v/v_0 = 1.5$ . [The slope of Eq. (20) differs slightly from  $\alpha$  at this velocity.] The constant  $\alpha$  was converted to sec using the densities of Be and Cu-Be. The result was

$$\begin{aligned} \alpha_{\text{Be}} &= (5.4 \pm 0.5) \times 10^{-13} \text{ sec}, \\ \alpha_{\text{Cu}} &= (3.3 \pm 0.25) \times 10^{-13} \text{ sec}, \end{aligned} \quad (26)$$

$$f = \alpha_{\text{Be}}/\alpha_{\text{Cu}} = 1.64 \pm 0.15.$$

Note that these stopping times are slightly different from what they would be for Eq. (19) or for  $R = \alpha v$ .

The attenuation factors for Be and Cu were evaluated by iteration. First  $\delta$  was assumed to be zero and  $\lambda\alpha_{\text{Cu}}$  was found from the experimental value for  $F_{\text{Cu}}$  (Sec. III), and  $\lambda\alpha_{\text{Be}}$  from  $\lambda\alpha_{\text{Be}} = f\lambda\alpha_{\text{Cu}}$ . Then  $\delta$  was evaluated taking  $v_i$  as  $c(\beta_i)$  (see Sec. III) and  $\lambda\alpha$  was redetermined from Eq. (22). Two repetitions of this procedure were sufficient. Finally, a rough plot of the distribution in intensity of  $\beta(0)$  was constructed from the available data for the two experimental conditions (Sec. III) and  $\delta$  was averaged over these distributions numerically using the values of  $\lambda\alpha$  determined from  $v_i = c(\beta_i)$ . This procedure resulted in  $\delta_{\text{Cu}} = (0.065 \pm 0.01)$  and  $\delta_{\text{Be}}$

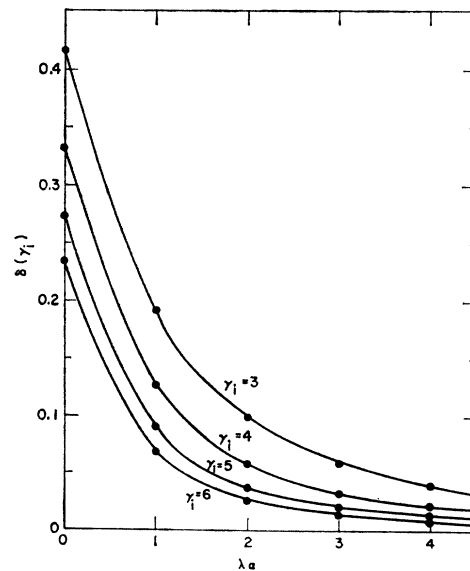


FIG. 10. The correction factor  $\delta(\gamma_i)$  as a function of  $\lambda\alpha$  for four values of  $\gamma_i$ .

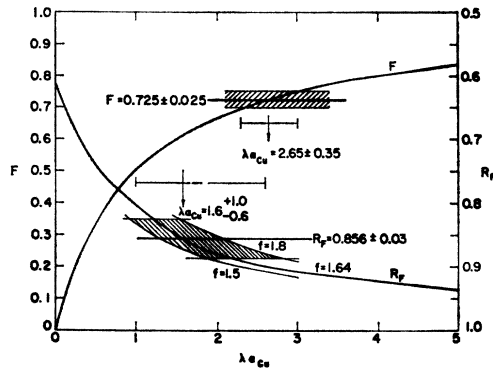


FIG. 11. The factors  $F$  and  $R_F$  as a function of  $\lambda\alpha_{Cu}$ . The experimental measurements of these factors and the resulting values of  $\lambda\alpha_{Cu}$  are also indicated. In the case of the determination of  $\lambda\alpha_{Cu}$  from the measurement of  $R_F$  the uncertainty in  $\lambda\alpha_{Cu}$  due to the uncertainty in  $f$  ( $=1.64\pm 0.15$ ) is indicated separately from that due to the experimental measurement.

$= (0.018\pm 0.003)$  for the first method and  $\delta_{Cu} = (0.042\pm 0.003)$  for the second method.

Applying these correction factors to the results of the last section gives

$$R_F = (0.816\pm 0.028) \left[ \frac{0.982\pm 0.003}{0.935\pm 0.001} \right] = (0.856\pm 0.03),$$

where  $R_F$  is defined by Eq. (11), and

$$F = (0.694\pm 0.024) / (0.958\pm 0.003) = (0.725\pm 0.025),$$

where  $F$  is defined by Eq. (4). In Fig. 11,  $R_F$  and  $F$  are plotted against  $\lambda\alpha_{Cu}$  using Eqs. (4) and (12). The experimental values of  $R_F$  and  $F$  are also shown in Fig. 11. For  $R_F$  the effect of the uncertainty in  $f$  is indicated as well as the uncertainty in the measurement of  $R_F$ . As indicated in Fig. 11, the measurement of  $F$  yields  $\lambda\alpha_{Cu} = 2.65\pm 0.35$  while the measurement of  $R_F$  leads to  $\lambda\alpha_{Cu} = 1.6_{-0.6}^{+1.0}$ .

The measurement of  $F_{Cu}' \langle \beta_i \rangle_{Cu} = (0.417\pm 0.013) \times 10^{-2}$  and the estimate of  $\langle \beta_i \rangle_{Cu} = (0.67\pm 0.1) \times 10^{-2}$  which were obtained as by-products in the determination of  $R_F$  also give some information concerning  $\lambda\alpha_{Cu}$ .

Taking the ratio of these values gives  $F_{Cu}' = 0.62\pm 0.10$  and using  $\delta(\gamma_i) = 0.065\pm 0.01$  gives  $F_{Cu} = 0.66\pm 0.10$ , corresponding to  $\lambda\alpha_{Cu} = 1.95_{-0.65}^{+1.2}$ . This result is consistent with the value of  $\lambda\alpha_{Cu}$  obtained from  $R_F$  and just about as accurate in spite of the rather large uncertainty in the estimate of  $\langle \beta_i \rangle_{Cu}$ . A large part of the uncertainty in the value of  $\lambda\alpha_{Cu}$  obtained from the measurement of  $R_F$  is due to the uncertainty in  $f$  ( $\equiv \alpha_{Be}/\alpha_{Cu}$ ) since  $R_F$  is quite sensitive to  $f$ . For this reason the first method we have described has inherently poor accuracy unless accurate stopping power data are available for the two stopping materials used.

Combining the values of  $\lambda\alpha_{Cu}$  obtained by the two methods with the value of  $\alpha_{Cu}$  given in Eq. (26) gives

$$\tau = (2.0\pm 1.0) \times 10^{-13} \text{ sec},$$

from the first method and

$$\tau = (1.3\pm 0.2) \times 10^{-13} \text{ sec},$$

from the gamma-gamma coincidence method. If a linear range-velocity relationship had been assumed, i.e.,  $R = \alpha c \beta(t)$ , then the two methods would have yielded mean lifetimes 50 and 13% higher, respectively. The two mean lifetimes are consistent with each other and we adopt

$$\tau = (1.4\pm 0.3) \times 10^{-13} \text{ sec},$$

for the mean lifetime of the  $Be^{10}$  first excited state. The uncertainty has been increased by about 50% to include possible systematic errors. This lifetime corresponds to a radiative width  $\Gamma_{\gamma \text{ exp}} = (4.7\pm 1.0) \times 10^{-3} \text{ eV}$ .

The present result is consistent with the limit,  $\tau < 3 \times 10^{-13} \text{ sec}$ , set by Kohler<sup>4</sup> but in disagreement with the limit,  $\tau < 8 \times 10^{-14} \text{ sec}$ , set by Boyarkina and Tulinov.<sup>8</sup> The latter limit which corresponds to a 67% confidence limit, resulted from a complicated experiment which was difficult to analyze; also, if the latest range-velocity data<sup>17-20</sup> are used to re-evaluate the stopping time of  $Be^{10}$  in Al which enters into an analysis of this limit, the 67% confidence limit becomes compatible with our result. Thus, we do not feel that the disagreement is too serious.